Altered cellular dynamics and endosteal location of aged early hematopoietic progenitor cells revealed by time-lapse intravital imaging in long bones

Anja Köhler,[1] Vince Schmithorst,[2] Marie-Dominique Filippi,[3] Marnie A. Ryan,[3] Deidre Daria,[3,4] Matthias Gunzer,[1] and Hartmut Geiger[3,4]

[1]Institute of Molecular and Clinical Immunology, Otto von Guericke University, Magdeburg, Germany; [2]Imaging Research Center and [3]Division of Experimental Hematology and Cancer Biology, Cincinnati Children's Hospital Medical Center, OH; and [4]Department of Dermatology and Allergic Diseases, Aging Research, University of Ulm, Ulm, Germany

Aged hematopoietic stem cells (HSCs) are impaired in supporting hematopoiesis. The molecular and cellular mechanisms of stem cell aging are not well defined. HSCs interact with nonhematopoietic stroma cells in the bone marrow forming the niche. Interactions of hematopoietic cells with the stroma/microenvironment inside bone cavities are central to hematopoiesis as they regulate cell proliferation, self-renewal, and differentiation. We recently hypothesized that one underlying cause of altered hematopoiesis in aging might be due to altered interactions of aged stem cells with the microenvironment/niche. We developed time-lapse 2-photon microscopy and novel image analysis algorithms to quantify the dynamics of young and aged hematopoietic cells inside the marrow of long bones of mice in vivo. We report in this study that aged early hematopoietic progenitor cells (eHPCs) present with increased cell protrusion movement in vivo and localize more distantly to the endosteum compared with young eHPCs. This correlated with reduced adhesion to stroma cells as well as reduced cell polarity upon adhesion of aged eHPCs. These data support a role of altered eHPC dynamics and altered cell polarity, and thus altered niche biology in mechanisms of mammalian aging. (Blood. 2009;114: 290-298)

Introduction

Tissues depend on stem and progenitor cells to sustain homeostasis in response to attrition, aging, or upon organ injury.[1] One of the best studied of these systems is hematopoiesis, in which functional, differentiated blood cells are generated from hematopoietic stem and progenitor cells (HSPCs).[2] In adult mammalians, hematopoiesis is primarily confined to the bone marrow (BM) cavities.[3,4] HSPCs and differentiated blood cells interact with nonhematopoietic cells in the BM, referred to as stroma cells providing a niche to these cells. Both a vascular as well as an endosteal niche have been identified for hematopoietic stem cells.[5-7] There is general agreement that the interaction of the hematopoietic cells with the stroma or microenvironment is central to hematopoiesis as it regulates cell proliferation, self-renewal, differentiation, and migration.[8,9]

Impaired hematopoiesis in aged individuals is thought to be at least in part a consequence of the aging of stem cells.[10-12] Hematopoietic stem cells (HSCs) from aged animals have a decreased per cell repopulation activity, are impaired in their support of erythropoiesis, and present with a skewing toward myeloid over lymphoid differentiation.[13] Aging of HSCs is partly stem cell intrinsic.[13-15] Multiple cellular and molecular mechanisms have been implemented in hematopoietic stem cell aging.[16-18] We recently postulated that aged in contrast to young primitive hematopoietic cells present with altered, less favorable interactions with the niche, which might in part explain impaired hematopoiesis in aged individuals.[19,20]

We thus developed time-lapse multiphoton intravital microscopy (MP-IVM) in long bones to determine the dynamics of young and aged hematopoietic cells inside the BM cavity. Imaging of HSC in the BM has only very recently become possible in the calvaria in vivo[6] or in explanted tibiae.[7] However, these studies did not address the biology of aged versus young cells, and it is still not clear whether situation in the calvaria is representative of the marrow in long bones.[6] Besides introducing a valid approach for intravital imaging of individual cells within long bones, we identified that differentiated hematopoietic cells like macrophages and dendritic cells (DCs) residing in BM are motile, while they show a distinct localization with respect to the endosteal surface. Secondly, we report that young early hematopoietic progenitor cells (eHPCs), although remaining fixed on the spot, present with constantly ongoing cell protrusion movements indicating synapse-like interactions with stroma cells in the diaphyseal regions on long bones in vivo, and that hematopoietic progenitor cells (HPCs) and eHPCs are found in distinct locations relative to the endosteum. Finally, our data show that aged eHPCs display a higher cell protrusion activity and are localized more distantly from the endosteum compared with young eHPCs, although showing reduced adhesion to stroma cells and presenting with a reduced number of polarized cells upon adhesion. These results provide insights into the dynamics and physiology of aged primitive cells in the marrow of long bones in vivo that might form a rational basis to

Submitted December 23, 2008; accepted March 22, 2009. Prepublished online as *Blood* First Edition paper, April 8, 2009; DOI 10.1182/blood-2008-12-195644.

An Inside *Blood* analysis of this article appears at the front of this issue.

The online version of this article contains a data supplement.

The publication costs of this article were defrayed in part by page charge payment. Therefore, and solely to indicate this fact, this article is hereby marked "advertisement" in accordance with 18 USC section 1734.

explain the reduced hematopoietic performance of aged individuals. The technologies developed in this study will ultimately support the characterization of the dynamics of stem cell synapses in long bones in vivo and their role in stem cell aging.

Methods

Animals

Young (2-4 months of age) C57BL/6J mice were obtained from The Jackson Laboratory and subsequently housed in the animal barrier facility at Cincinnati Children's Hospital Medical Center (CCHMC) or the facility of the Helmholtz Center for Infection Research (HZI) or the Otto-von-Guericke University (OvGU). Aged C57BL/6J (18-20 months of age) animals were retired breeders derived from our own colony or obtained from the National Institute on Aging aged rodent colony (Harlan). Animals transgenic for yellow fluorescent protein (YFP) under the 2.3-kb fragment of the Col1a promoter were provided by R. Wenstrup (Cincinnati, OH). Green fluorescence protein (GFP) mice,[21] provided by S. Jung (Rehovot, Israel), were bred in OvGU facilities. All animals were housed in a pathogen-free environment in the CCHMC barrier facility or at the HZI or OvGU. All animal experiments were approved by the Institutional Animal Care and Use Committee at CCHMC by the Gewerbeaufsichtsamt Braunschweig and by the Landesverwaltungsamt Sachsen-Anhalt.

Isolation and staining of HPCs and eHPCs

LIN^-, c-Kit^+, Sca-1^+ (HSCs), and LIN^-, c-KIT^+, Sca-1^- (HPCs) were isolated according to standard protocols using a BD FACSVantage cell sorter (BD Biosciences) or a MoFlo cell sorter (Dako Deutschland GmbH), as described previously.[22] The LIN mixture contained anti-CD11b (clone M1/70), anti-B220 (clone RA3-6B2), anti-CD5 (clone 53-7.3), anti-Gr-1 (clone RB6-8C5), anti-Ter^{119}, and anti-CD8a (clone Ly-2), all from BD Biosciences. Isolated cells were stained with either carboxyfluorescein succinimidyl ester (CFSE) or Cell Tracker Orange (CTO; both Molecular Probes) for 1 hour in phosphate-buffered saline (PBS), according to previously published protocols.[23] Sorted cells were injected into a single mouse each (between 0.84 and 1.2×10^6 $L^-S^-K^+$ cells and 0.65 and 1.3×10^5 $L^-S^+K^+$ cells from young donors per recipient, and between 1.2 and 2.0×10^6 $L^-S^-K^+$ cells and 1.96 and 3.5×10^5 $L^-S^+K^+$ cells from aged donors per recipient).

Intravital microscopy

Mice were prepared for intravital microscopy using isofluran-based intubation narcosis, as described in detail in Figure 1 and previously.[23,24] Subsequently, the tibia was exposed by removing the skin on top of the bone, and further removing muscle tissue with a scalpel. Bone tissue was subsequently carefully removed with an electric drill (Dremel) to obtain a very thin (~ 30-50 μm) remaining layer of bone tissue covering the BM cavity, thus permitting better light penetration. This procedure was permanently controlled by stereomicroscopy to maintain the necessary thickness of the remaining bone tissue. Two-photon microscopy on the tibia was subsequently performed, as previously described,[24,25] using a customized 2-photon microscope (TrimScope; LaVision BioTec) with detection either by a charge-coupled device (CCD) camera (multifocal illumination) or an array of independent photo-multiplier tubes (PMT) detectors (single-point illumination). Bone tissue was identified due to its strong autofluorescence (CCD) under unfiltered light conditions or using its second-harmonic (SHG) signal (PMT). Animals were kept at 37°C in a PBS water bath while experiments were performed. For imaging, a 300×300-μm area was scanned in 30 steps of 4 μm down to 120 μm depth (~ 12 cell layers) using an illumination wavelength of either 800 or 880 nm detecting green (530 nm) and red (580 nm) fluorescence, as well as unfiltered light or SHG (at 480-nm emission). This sequence was repeated every 60 to 80 seconds for a total of up to 60 minutes.

Cobblestone area-forming cell adhesion assay

The cobblestone area-forming cell adhesion assay to measure the ability of hematopoietic stem and progenitor cells to the established murine preadipose female BM-derived 1 (FBMD-1) stroma cell line were performed, as previously described.[19]

Expression of adhesion receptors

For the determination of the expression of adhesion receptors, low-density BM cells were individually incubated with biotinylated antibodies (BD Biosciences) specific for either CD184 (clone 2B11/CXCR4), CD49d (clone R1-2), CD49e (clone 5H 10-27), CD106 (clone 429), CD62L (clone MEL-14), CD44 (clone IM7), or platelet endothelial cell adhesion molecule-1 (PECAM-1; clone 390), and subsequently with phycoerythrin (PE)–labeled LIN^- mixture antibodies (anti-CD3ϵ [clone 145-2C11], anti-B220 [clone RA3-6B2], anti-CD11b [clone M1/70], and anti-Gr-1 [clone RB6-8C5]; all from BD Biosciences); anti-Sca-1 PE-Cy7 (eBiosciences); and anti-c-Kit allophycocyanin and streptavidin fluorescein isothiocyanate (BD Biosciences).

Generation of movies and determination of the distance to endosteum

Primary data from the CCD camera were imported into the Volocity Software package (Version 4.3; Improvision) for further processing and conversion into 3-dimensional movies. Movies were then exported into the .avi format. Volocity software was also used to determine the distance of the cells from the endosteum.

Determination of cell movement

The motility of cells inside the BM was determined, as recently described, using a self-programmed cell-tracker software.[26]

Determination of protrusion movement

To determine the changes in cell surface area as well as a cell volume of CFSE-stained cells, novel algorithms were developed using the IDL software suite from ITT (see supplemental Experimental Procedures, available on the *Blood* website; see the Supplemental Materials link at the top of the online article).

Polarity staining

Sorted cells ($LIN^-S^+K^+$ or $LIN^-S^-K^+$ at 5×10^3 each) were cultured on slides coated with 50 ng/mL fibronectin in Iscove modified Dulbecco medium containing 10% fetal calf serum, stem cell factor, granulocyte colony-stimulating factor (G-CSF), and megakaryocyte growth and development factor (100 ng/mL each) for 14 hours at 37°C. The cells were then fixed with 2% paraformaldehyde containing NaCl and $Mg^{2+}Cl_2$ for 20 minutes at 37°C. The cells were then treated with 0.1% Triton for 5 minutes and stained with anti–mouse anti–α-tubulin and anti–mouse anti–β-tubulin for 1 hour at 37°C, followed by anti–mouse Alexa 488 (Molecular Probes) rhodamine-labeled phalloidin (Molecular Probes) for 1 hour at room temperature. Z series of fluorescence images were captured using a Leica DMIRB fluorescence microscope (Leica Microsystems) at 63× magnification with ORCA-ER C4742-95 camera (Hamamatsu) equipped with a deconvolution system (Leica Microsystems) driven by Openlab software. Z series were then analyzed by deconvolution using Volocity software.[27,28] Scoring cells for polarity were based on 3 criteria: (1) shape of the cell (elongated/drop shaped [polar] vs nonhomogeneous [nonpolar]); (2) the distribution of F-actin and the corresponding membrane ruffles are asymmetric (polar) versus more symmetric (nonpolar); and (3) distribution of the microtuble network, in which localization opposite the F-actin network characterizes a polar cell.

Statistics

A paired Student *t* test was used to determine the significance of the difference between means, except for the densitometry analyses of the

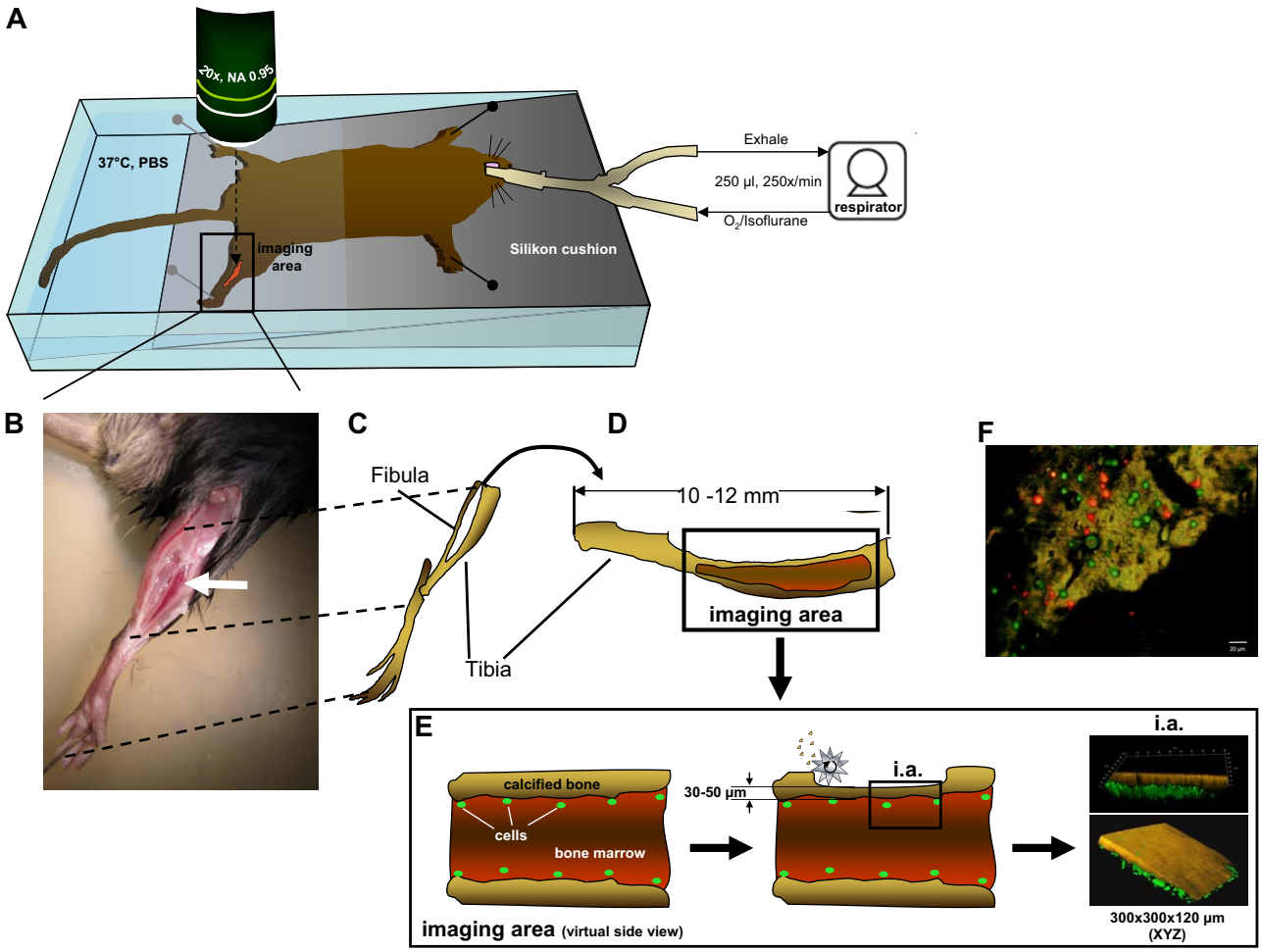

Figure 1. Imaging hematopoietic cell movement in the tibial BM of a live mouse. (A) Setup of the mouse in the imaging chamber. The animal is ventilated through a tracheal tubus by a mechanical small animal respirator receiving a mixture of O_2/isoflurane for narcosis at the depicted rates and volumes. The gross area of bone thinning and imaging is boxed and the approximate position of the microscope lens is indicated with a dashed arrow. Imaging is performed anywhere within the red (thinned) area of the tibia. All fluorescently marked cells detectable within this area are recorded by individual Z-stacks. (B) A close-up micrograph of a mouse fixed for imaging with the position of the tibia indicated (white arrow). (C) Drawing of the bones of the hind leg as they are positioned for the animal shown in panel B. (D) Enlargement of the tibial bone, rotated 90° clockwise with the area of preparation indicated by the red color. (E) Virtual side view through the tibial bone in the area of imaging to demonstrate the process of careful bone thinning by an electric drill (silver star), which is constantly monitored with a stereomicroscope until finished. The residual bone surface is kept at 30 to 50 μm thickness, whereas a nondrilled tibia has a wall thickness of approximately 100 μm. Of note: extreme care has to be taken to not totally remove the covering bone. If this happens, the contents of the BM will leak out, rendering imaging impossible in a live mouse with intact blood circulation. The figure on the right shows as an example rendered images of a bone with fluorescently labeled (green) cells below the bone surface. The typical XYZ dimensions of the area of imaging are depicted. (F) To demonstrate the practicability of the transplantation/visualization technique, BM cells were stained with CFSE (green) or CTO (red) and transplanted together in equal numbers in recipient animals. Cells were visualized by 2-photon intravital microscopy in the region close to the endosteum in the tibia (brown = autofluorescence signal of the calcified bone) 16 hours postinjection. The corresponding movie is available as supplemental Video 1.

movies, which were analyzed according to methods described in the supplemental Experimental Procedures.

Results

Dynamics of differentiated hematopoietic cells in the murine tibia

The structural components of potential stem and progenitor cell niches might be distinct for different types of bones and tissues.[6,29,30] In this context, it is important that most intravital analyses of the localization of hematopoietic cell to date have been performed on cells within blood vessels or the BM matrix of the calvarium (skull bones[6,30-32]). In contrast, HSCs for molecular and functional analyses are usually derived from the marrow of long bones. We thus established MP-IVM in the murine tibia to visualize primitive hematopoietic cells in the vicinity of the endosteum of this long bone (see Figure 1 and description of technical details in the figure legend as well as in supplemental Figure 1). To optimize the cell/transplantation imaging system, unfractionated BM was labeled with either CFSE or CTO and cotransplanted into recipient animals. Fluorescently labeled cells inside the bone cavity were analyzed by MP-IVM 16 hours posttransplantation (Figure 1F and supplemental Video 1), demonstrating visualization of active cell dynamics of the transplanted cells in the region close to the endosteum. MP-IVM achieved a penetration into long bones of up to 120 μm (Figure 1E).

Both macrophages and DCs are reported to be highly motile in peripheral organs in vivo.[33,34] In contrast, published data on the motility of hematopoietic cells in BM (ex vivo) suggested a low motile activity of these cells.[35] We therefore decided to investigate the dynamics and location of these 2 cell types in the BM cavity (Figure 2 and supplemental Video 2) using an established knockin CX3CR-GFP mouse model in which macrophages (MCs; white

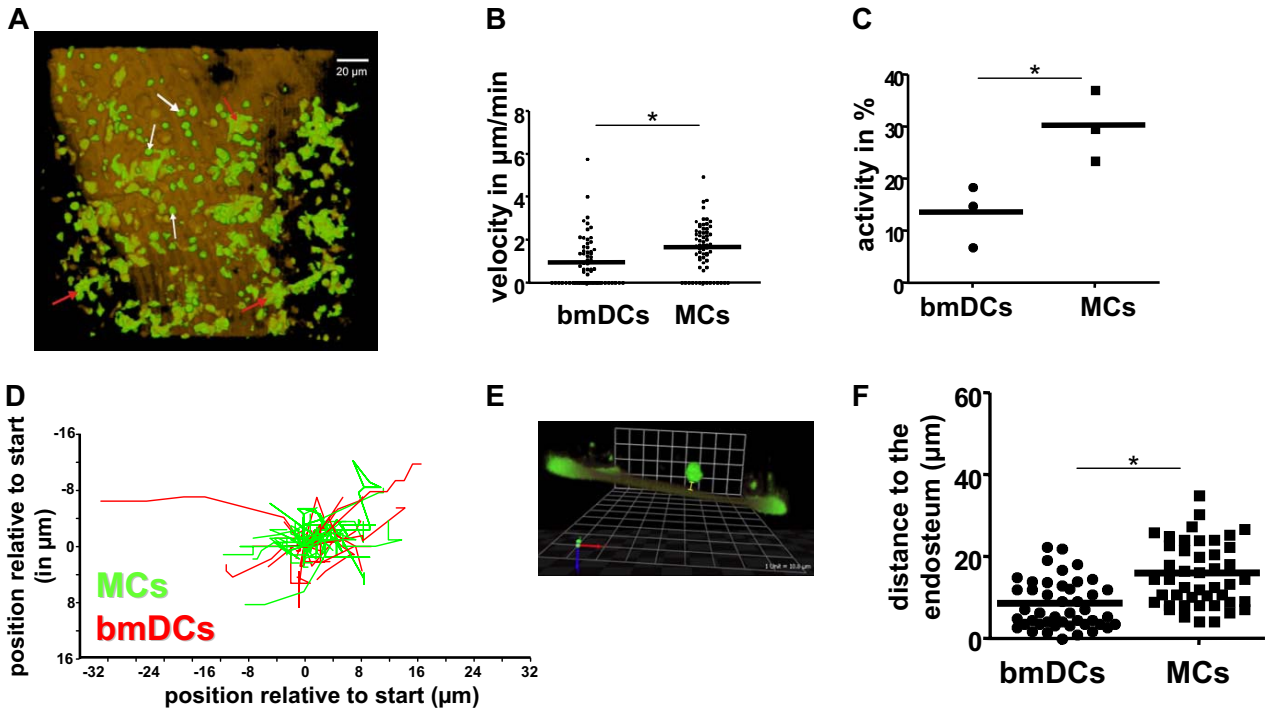

Figure 2. Time-lapse intravital microscopy of BMDCs and macrophages in the tibia. (A) Visualization of BMDCs (red arrows) and macrophages (MCs, white arrows) in the vicinity of the endosteum in vivo using the CX3CR-GFP mouse model, in which these cell types are green. The brown color delineates the SHG signal of the calcified bone (the corresponding movie is available as supplemental Video 2). (B) Quantification of the velocity of BMDCs and MCs in the BM (n = 65 cells per cell type, based on 3 independent experiments). (C) Activity (eg, percentage of cells that present with cell position changing migration) of BMDCs and MCs in the BM, based on 3 independent experiments. (D) Trajectories of individual BMDC and MC movement (n = at least 10 per cell type). (E) Schematic of the grid approach to quantify the distance of the cells to the endosteum, as described in "Methods." A CFSE-stained transplanted cell (green) is shown in a side view to demonstrate its distance to the calcified bone (brown, autofluorescence). The yellow scale bar from the lower part of the cell body to the bone surface represents the distance to the endosteal surface measured for this cell. All cells were analyzed analogously to obtain distance values. (F) Distance of BMDCs and MCs to the endosteum (vertical bars representing average, n = 65 cells per cell type, based on 3 independent experiments). *$P < .05$.

arrows in Figure 2A) and BMDCs (red arrows in Figure 2A) are identified by a combination of fluorescence and cell shape.[21,36-38] BMDCs (green cells with dendritic morphology) presented in cell clusters (Figure 2A) imply the existence of direct cell-cell communication between individual DCs in the BM. In contrast, MCs (small green cells with round morphology) were more solitary, although showing a significantly elevated spontaneous cell motility (1.6 vs 0.9 μm/min; Figure 2B) with an overall higher cell activity (percentage of cells that show migration; Figure 2C). Velocities for MCs and DC previously observed in 3-dimensional collagen lattices (2.0 μm/min for MCs vs 1.2 μm/min for DCs) are similar, but not identical to the velocity in BM in vivo.[39] The migration patterns for both cell types under these steady-state conditions were nondirectional (Figure 2D), implying that the migration is spontaneous and not guided by a gradient. Determining the distance to the bone (Figure 2E and technical details in supplemental Figure 1), both MCs and BMDCs were found in close vicinity to the endosteal layer of the BM (distance to the bone in μm: DCs 8.2 and MCs 15.6; Figure 2F), but rarely in direct contact with the endosteum. In summary, MCs and BMDCs inside the BM are motile and are found in a region close to the endosteum. The especially close location of clusters of BMDCs relative to the endosteum (less than a cell diameter) might suggest a role for BMDCs in the physiology of the endosteum.[36]

Quantification of cell protrusion movement and localization of young primitive hematopoietic cells in long bones in vivo

To investigate the dynamics of HSPCs, in vivo sorted and fluorescently labeled cell populations enriched for HPCs ($LIN^-S^-K^+$ cells) and eHPCs ($LIN^-S^+K^+$ cells) were transplanted individually into syngeneic recipient animals and analyzed by MP-IVM between 18 and 36 hours after transplant (Figure 3A-B) using the established lodgement assay.[7,40,41] Transplanted $L^-S^-K^+$ as well as $L^-S^+K^+$ cells were consistently found in close vicinity to the endosteum (Figure 3A-B). Dye exchange experiments were performed to exclude label-specific influences on the localization of $L^-S^+K^+$ cells (supplemental Figure 2A). Some cells were directly attached to the endosteum (Figure 3C), although displaying extended protrusions upon attachment (Figure 3C). As we have not seen any HPC or eHPC cell cluster to date ($n > 50$ for eHPCs and $n > 100$ for HPCs), we conclude that primitive hematopoietic cells reside solitarily in their BM niche. In contrast to macrophages and DCs (Figure 2B-D), HPCs and eHPCs were completely immobile (data not shown). Both cell types though showed constantly proceeding protrusion movements of the cell periphery, suggesting that they actively and reversibly engage the microenvironment (supplemental Video 3, $L^-S^-K^+$ cells; supplemental Video 4, $L^-S^+K^+$ cells). To mathematically quantify the extent of cell protrusion movement over time, we developed algorithms to calculate both the change in volume and the surface area over time of the observed cells based on the data obtained from the MP-IVM (technical and mathematical details listed in supplemental Experimental Procedures). These analyses revealed that both $L^-S^-K^+$ as well as $L^-S^+K^+$ cells presented with active cell protrusion movement indicated by absolute changes in cell volume between time points (Figure 3D) as well as by the variance in change in cell volume (Figure 3E) and the variance in the change in cell surface area (Figure 3F). The variance is a measure of how spread out a

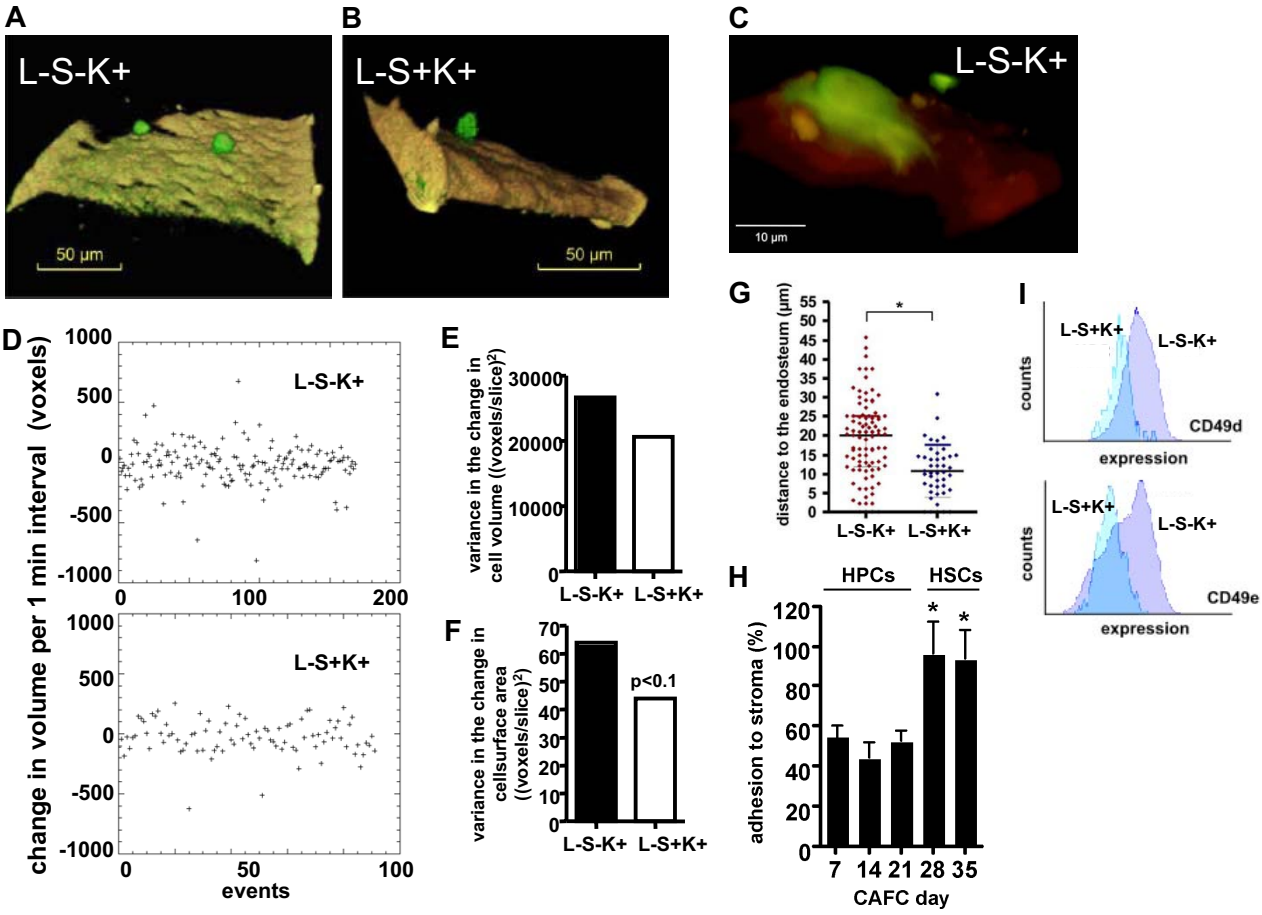

Figure 3. CFSE-labeled HPCs (Lin$^-$, Sca-1$^-$, c-Kit$^+$; L$-$S$^-$K$^+$) or eHPCs (Lin$^-$, Sca-1$^+$, c-Kit$^+$; L$-$S$^+$K$^+$) were transplanted in recipient animals. The tibia of recipient animals was analyzed between 16 and 40 hours posttransplant by intravital time-lapse 2-photon microscopy to monitor CFSE-labeled green (A) L$^-$S$^-$K$^+$ cells and (B) L$^-$S$^+$K$^+$ cells close to the endosteal region (brown signal, autofluorescence) of the bone. (C) Example of cell protrusions extending from transplanted L$^-$S$^-$K$^+$ cells into the endosteum (green = CFSE, brown/red = bone surface [autofluorescence]). (D) Quantification of cell protrusion movement, determined as the change in volume over time (interval of 1 minute) of transplanted L$^-$S$^-$K$^+$ and L$^-$S$^+$K$^+$ cells, as described in supplemental Experimental Procedures (n = 169 changes for L$^-$S$^-$K$^+$ cells and n = 92 changes for L$^-$S$^+$K$^+$, based on at least 3 independent experiments for each cell population; see also as example supplemental Video 3 for L$^-$S$^-$K$^+$ cells and Video S4 for L$^-$S$^+$K$^+$ cells). (E) Average variance in the change in cell volume in a 1-minute time interval of L$^-$S$^-$K$^+$ and L$^-$S$^+$K$^+$ cells (n = 169 changes for L$^-$S$^-$K$^+$ and n = 92 changes for L$^-$S$^+$K$^+$, based on at least 3 independent experiments for each cell population). (F) Average variance in the change of cell surface area in a 1-minute time interval of L$^-$S$^-$K$^+$ and L$^-$S$^+$K$^+$ cells (n = 169 changes for L$^-$S$^-$K$^+$ and n = 92 changes for L$^-$S$^+$K$^+$, based on at least 3 independent experiments for each cell population). (G) Distance of L$^-$S$^-$K$^+$ cells and L$^-$S$^+$K$^+$ cells to the endosteum; each dot represents a single cell; black horizontal bars depict the average distance; and red/blue horizontal bars depict the standard deviation (n = 93 for L$^-$S$^-$K$^+$ and n = 44 for L$^-$S$^+$K$^+$, based on at least 3 independent experiments for each cell population). (H) Percentage of HPCs (CAFC day 7-21 cells) and HSCs (CAFC days 28 and 35 cells) that adhere in 3 hours to FBMD-1 stroma cells in vitro, determined by the CAFC adhesion assay. n = at least 6 experiments for each time point. (I) Relative level of expression of CD49d and CD49e on HPCs and HSCs as determined by flow cytometry. Figure is representative of 6 independent experiments. *$P < .05$.

distribution is. In other words, it is a measure of variability, representing the extent of the changes in volume or cell surface area/1 min. We also observed a trend for L$^-$S$^-$K$^+$ cells being more active with respect to changes in the cell surface area compared with L$^-$S$^+$K$^+$ cells. These observations are consistent with a hypothesis in which stem cells in general are more "quiet" and thus less dynamic compared with progenitor cells.

As anticipated from a model in which stem cells locate closer to the endosteum compared with more differentiated cells, our analysis revealed that 11% of transplanted L$^-$S$^+$K$^+$ cells had direct contact to the endosteum in the tibia, whereas only 4% of L$^-$S$^-$K$^+$ cells were in direct contact with the endosteum (Table 1). In addition, L$^-$S$^+$K$^+$ cells resided on average closer to the endosteum compared with L$^-$S$^-$K$^+$ cells (11 vs 19 μm; Table 1 and Figure 3G). L$^-$S$^+$K$^+$ cells were not randomly distributed in the region analyzed, as more than 95% of all L$^-$S$^+$K$^+$ cells were found to reside within 20 μm of the endosteum.

These data are consistent with recently published MP-IVM or real-time imaging analyses of stem cells in the calvarium or ex vivo BM[6,7] and support a model in which niches for L$^-$S$^-$K$^+$ cells are distinct from niches for L$^-$S$^+$K$^+$ cells and/or HPCs differ from eHPCs in the quality of interaction with stroma cells. Using a

Table 1. Summary of cell analysis

	Number of cells analyzed	Cells not directly attached to endosteum (%)	Cells attached to endosteum (%)	Average distance to endosteum, μm
Young L$^-$S$^-$K$^+$ (n = 6)	93	95.7	4.3	18.94
Young L$^-$S$^+$K$^+$ (n = 6)	44	88.6	11.4	10.72
Aged L$^-$S$^+$K$^+$ (n = 3)	50	88.0	12.0	18.05

cobblestone area-forming cell adhesion assay, we further tested these hypotheses, comparing the adhesive properties of HSCs and HPCs with respect to stroma cells.[42] In accordance with localization closer to the endosteum as well as less protrusion movement, both of which imply stronger and/or preferential adhesive capabilities, HSCs (CAFC day 28 and 35 cells) presented with significantly increased adhesion to the FBMD-1 stroma cells compared with HPCs (CAFC day 7, 14, and 21 cells; Figure 3H).

Adhesion molecules regulate the adhesion and localization of stem and progenitor cells.[3,4,43-46] We therefore performed flow cytometric analyses to measure the levels of surface expression of adhesion molecules reported to be involved in regulating hematopoiesis. $L^-S^+K^+$ cells, in comparison with $L^-S^-K^+$ cells, presented with a reduced level of expression of CD49d, CD49e (Figure 3I), as well as CD44 and PECAM-1 (data not shown), whereas the surface expression levels for the other adhesion molecules investigated (CD106, CXCR4, CD62L, CD44) were not significantly altered between the 2 cell types (data not shown). Paradoxically, these data show an inverse correlation between level of expression of CD49d and CD49e and distance to the endosteum, as well as intensity of protrusion movements.

Elevated cellular dynamics and distinct localization of aged eHPCs

Multiple cellular and molecular mechanisms have been implemented in hematopoietic stem cell aging.[16-18] We recently postulated that aged compared with young stem cells might present with altered, less favorable interactions with the niche, which could in part explain impaired hematopoiesis in aged individuals.[19,20] Using MP-IVM, we set out to verify this hypothesis. Upon transplantation, aged $L^-S^+K^+$ cells, similar to young $L^-S^+K^+$ cells, were detected at solitary spots along the endosteum (supplemental Video 5) and were immobile (data not shown). Interestingly, aged $L^-S^+K^+$ cells presented with significantly increased protrusion movements compared with young $L^-S^+K^+$ cells as indicated by (1) increased changes in volume between time points (Figure 4A) and a significantly ($P < 10^{-6}$; F test) increased (2) average variance in the change in cell volume (Figure 4B), as well as (3) average variance in the change of cell surface area (Figure 4C). Moreover, aged $L^-S^+K^+$ cells were located at sites more distant from the endosteum (average distance from the endosteum of 18.1 μm for aged compared with 10.7 μm for young; Table 1 and Figure 4D), with aged $L^-S^+K^+$ cells residing as far as 40 μm away from the endosteum. These data might thus imply that aged HCSs reside in distinct niches and/or interact with stroma cells with a distinct dynamic. To compare the ability of young and aged HSCs to adhere to stroma in vitro, a CAFC-adhesion assay was performed. Initial experiments supported that this assay is suitable to determine the adhesion ability of functionally defined primitive hematopoietic cells to stroma (supplemental Figure 2B). Aged HSCs (CAFC day 28 cells) displayed a significantly reduced adhesion to the FBMD-1 stroma cell line compared with young HSCs (Figure 4E), which was consistent with their elevated cell protrusion movement and their more distant localization from the endosteum. In some of our experiments, young and aged $L^-S^+K^+$ cells were transplanted in animals with YFP-positive osteoblasts located at the endosteum (supplemental Figure 3). Similar to observations in the calvarium,[6] neither young nor aged $L^-S^+K^+$ cells ($n > 20$ for both cell types) were directly associated with osteoblasts in long bones, implying in general an indirect influence of this cell type on hematopoiesis, whereas adjacent N-cadherin–positive preosteoblasts might directly interact with $L^-S^+K^+$ cells, as recently identified.[7]

The ability to polarize upon adhesion to stroma is tightly connected to the quality of adhesive cell-cell interactions.[47,48] In addition, altered cell polarity has been reported to play a role in aging in yeast.[49] We thus investigated the extent of polarization of young and aged $L^-S^+K^+$ cells upon adhesion to the matrix molecule fibronectin (Figure 4F). Using polarity of the actin and the microtubule cytoskeleton as a marker for cell polarization, aged $L^-S^+K^+$ cells presented with a significantly reduced ability to polarize (Figure 4F-G), which correlated with their reduced adhesion to stroma, the increased cell protrusion movement, and their altered localization in vivo. Finally, we compared the surface expression level of adhesion receptors on young and aged $L^-S^+K^+$ cells, focusing on the receptors that were differentially expressed between young $L^-S^+K^+$ and $L^-S^-K^+$ cells (Figure 3I). Expression of CD49d was reduced, whereas CD49e was elevated on aged $L^-S^+K^+$ cells (Figure 4H), with no significant changes in expression of CD44 and PECAM-1 (data not shown). In aggregation, these data demonstrate that aged eHPCs present with intrinsically elevated protrusion movements, correlating with reduced adhesive activity, a reduced frequency of polarized cells, and localization more distant from the endosteum. These data demonstrate interactions of aged eHPCs with the microenvironment that are distinct from young eHPCs, and imply this to be one underlying cause for the reduced self-renewal ability as well as the altered differentiation patterns of aged primitive hematopoietic cells.

Discussion

The dynamics of HSCs in the BM cavity are central to the regulation of stem cells. We recently postulated that aged stem cells compared with young present with altered, less favorable interactions with the niche, which might in part explain impaired hematopoiesis in aged individuals.[19,20]

Our observations using time-lapse MV-IVM are to the best of our knowledge the first analyses describing the in vivo short-term dynamics of young and aged HPCs and eHPCs and differentiated hematopoietic cells close to the endosteum in long bones. They revealed that young primitive hematopoietic cells present with active cell protrusion movement ("running on the spot") in long bones, although sustaining interactions with the microenvironment that are very dynamic (supplemental Videos 3 and 4; Figures 3D-F). The contact plane between T cells and antigen-presenting cells, which has been termed immunologic synapse (IS),[50] has been well defined both in vitro[23,50,51] and in vivo.[52,53] It has been hypothesized that the contact plane of primitive hematopoietic cells with the niche cells in the microenvironment is similar to the IS, and has thus been named stem cell synapse.[4,5,54] As can be deduced from our imaging analyses, such synapses might be less dynamic than early immunologic synapses, resembling more the slow second phase-type interactions of T cells with antigen-presenting DC during the adaptive immune response.[50,53,55-57]

Similarly to HPCs and eHPCs lodging to the niche in the calvarium[6] and as detected in ex vivo real-time imaging of lodged HSCs in the BM,[7] HPCs and eHPCs in long bones are also solitary and do not present with spontaneous migration after they reach a destination/location in vicinity to the endosteum.[6] Interestingly though, eHPCs seem to lodge closer to the endosteal surface in the diaphysis of long bones (reported in this study) compared with the lodging relative to the endosteal region in the calvarium.[6] This

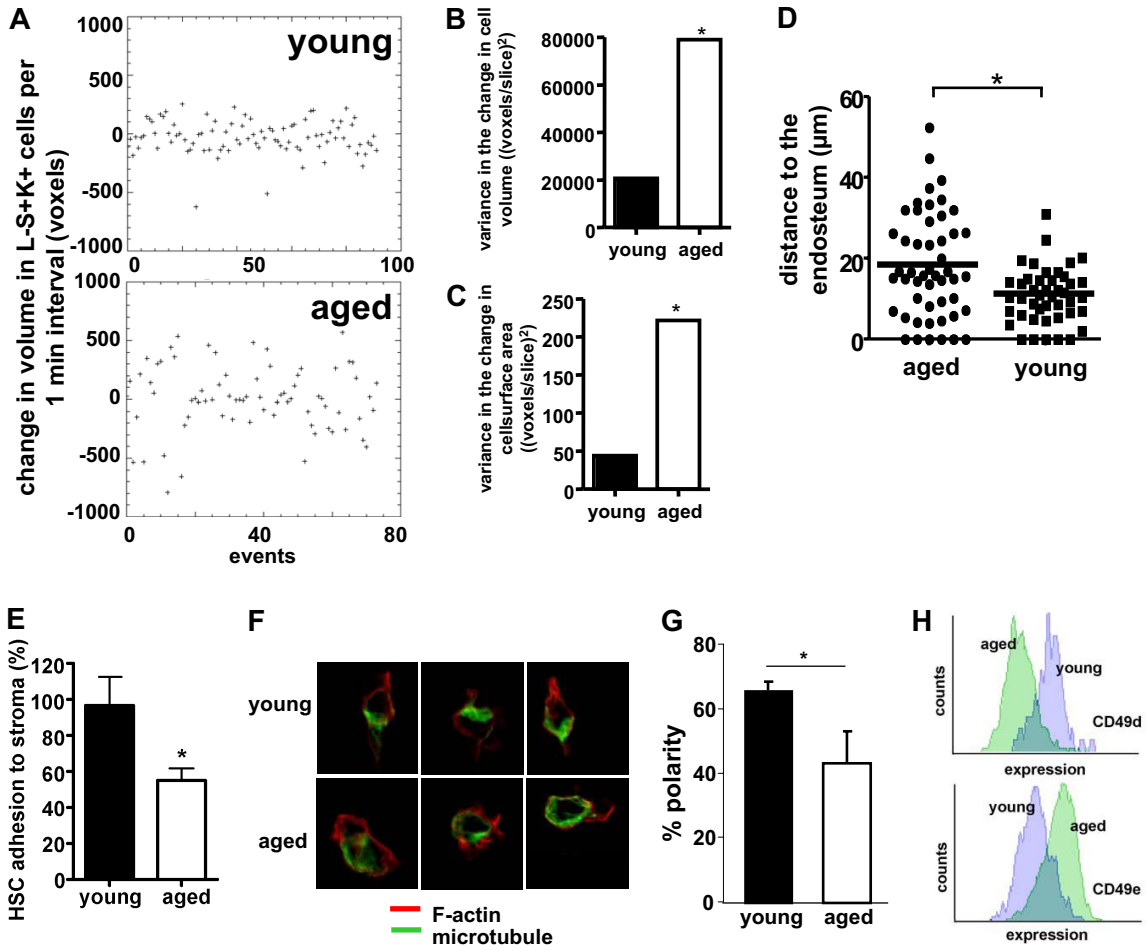

Figure 4. HSCs from aged mice (20- to 24-month-old animals) were fluorescently labeled (CFSE or CTO) and transplanted into young recipient animals. Tibiae from recipient animals were analyzed between 16 and 40 hours after transplantation. (A) Quantification of cell protrusion movement, determined as the change in volume over time (interval of 1 minute) of transplanted $L^-S^-K^+$ and $L^-S^+K^+$ cells, as described in supplemental Experimental Procedures (n = 92 changes for young $L^-S^+K^+$ cells and n = 74 changes for $L^-S^+K^+$ cells, based on at least 3 independent experiments for each cell population; see also as example supplemental Video 5 for aged $L^-S^+K^+$ cells in addition to supplemental Video 4 for young $L^-S^+K^+$ cells). (B) Average variance in the change in cell volume in a 1-minute time interval of $L^-S^-K^+$ and $L^-S^+K^+$ cells (n = 92 changes for $L^-S^-K^+$ and n = 74 changes for $L^-S^+K^+$, based on at least 3 independent experiments for each cell population). (C) Average variance in the change of the cell surface area in a 1-minute time interval of $L^-S^-K^+$ and $L^-S^+K^+$ cells (n = 92 changes for $L^-S^-K^+$ and n = 74 changes for $L^-S^+K^+$, based on at least 3 independent experiments for each cell population). (D) Distance of young and aged transplanted $L^-S^+K^+$ cells to the endosteum; black horizontal bars depict the average distance (n = 44 for young $L^-S^+K^+$ cells and n = 50 for aged $L^-S^+K^+$ cells, based on at least 3 independent experiments for each cell population). (E) Percentage of young and aged HSCs (CAFC day 28 cells) that adhere to FBMD-1 stroma cells in vitro, determined by the CAFC adhesion assay (n = 6 experiments). (F) Cytoskeletal cell polarity in young and aged HSCs (Lin^-, Sca-1^+, c-Kit^+) upon adhesion to fibronectin (determined by staining for F-actin [red] and microtubules [green]). (G) Percentage of polar aged and young HSCs upon adhesion (quantification of data from panel F; n = 3 with at least 20 cells analyzed per experiment). (H) Level of expression of CD49d and CD49e on young and aged HSCs as determined by flow cytometry. Figure is representative of 6 independent experiments. *$P < .05$.

might indicate a distinct niche architecture in long bones compared with calvarium.

Imaging in the CX3CR1-enhanced EGFP knockin mouse clearly demonstrated that the region close to the endosteum is not exclusively occupied by undifferentiated hematopoietic cells, further emphasizing the complexity of the BM environment. Because both macrophages and DCs (Figure 2B-D) are highly motile, we conclude that migration of primitive hematopoietic cells is not hampered by a physical barrier close by the endosteum. Rather, HPCs and eHPCs either actively suppress migration once they reach their destination or the activity of cytokines that might be able to support eHPC migration, like stromal cell–derived factor 1 (SDF-1), might be restricted to very distinct locations in vivo. The latter hypothesis is supported by the finding that stroma cells expressing SDF-1 (CXC chemokine ligand 12), which can induce migration in primitive hematopoietic cells,[58] are distributed in a spotty manner inside the bone.[59]

Aging of stem cells is regarded to be involved in impaired tissue homeostasis in organs that rely on stem cell activity.[12] Several models of stem cell aging exist to explain the reduced proliferative and regenerative capacity of aged stem cells, including DNA damage, action of reactive oxygen species, and/or telomere attrition.[10,20,60,61] Our observations support a model in which altered cell polarity and localization as well as altered cell-cell interactions of aged eHPCs might alter the quality of the interaction of aged primitive hematopoietic cells with the niche, causing the phenotypes associated with aged eHPCs. As stem cell-stroma interactions are instrumental in determining stem cell self-renewal and stem cell differentiation, altered interactions will most likely result in altered differentiation/self-renewal outcomes.

Surprisingly, elevated levels of expression of the α_5 integrin chain (CD49e) correlated with reduced adhesion to stroma cells as well as more distant localization from the endosteum for young and aged cells. This might imply that the level of expression of α_5

integrin is a modifier of localization of primitive hematopoietic cells with respect to the endosteum and might regulate which microenvironment (niche) a cell will reside in upon transplantation. An influence of α_5 integrins on stem cell niche interactions is consistent with the fact that (1) blocking α_5 integrins on HSCs reduces homing to the BM, but not the spleen (which does not have endosteal structures;[62-64] (2) α_5 integrins regulate engraftment of human hematopoietic stem and progenitor cells;[65] and (3) the cell surface expression level is increased in BM-resident HSCs during the course of mobilization by G-CSF.[66] Very late activation antigen 5 (VLA5; the α_5, β_1 integrin heterodimer) binds to the ubiquitous extracellular matrix molecule fibronectin, but also to ligands like osteopontin, thrombospondin, a disintegrin-like and metalloprotease (ADAM) family members, and cartilage oligomeric matrix protein.[67] Thus, these ligands might play a role in directing stem cells to their location via its interaction with VLA5, and might thus be tightly associated with niches in vivo, but might also play a role in stem cell aging. For example, osteopontin was recently identified as a possible regulator of the distribution of HSCs in the BM posttransplantation.[68,69]

Our data leave the question open to which cells eHPCs entertain direct cell-cell contact. We predict that using novel animal strains in which additional types of hematopoietic[70] or stroma cells are fluorescently labeled will result in further information on cell-cell interactions in stem cell synapses in long bones, and will allow us to monitor both the endosteal and the perivascular endothelial region within long bones and their influence on aging, similarly to recently published ex vivo analyses of functional stem cell niches in the femur.[7]

In summary, using time-lapse MP-IVM to visualize hematopoietic cells inside the BM cavity of long bones, we present experimental evidence for the existence of eHPC cell synapses within the niche. In addition, our data imply distinct primitive hematopoietic cell stroma interactions for aged eHPCs that might impact on both their self-renewal and differentiation potential, probably similar to mechanisms recently described for aged germline stem cells in *Drosophila*.[71] We anticipate that time-lapse MP-IVM in long bones will open up new avenues for the investigation of mammalian stem cell biology in vivo.[72]

Acknowledgments

We thank Jose Cancelas, Lee Grimes, and Yi Zheng for discussions and the critical comments on the manuscript, and the Comprehensive Mouse and Cancer Core at CCHMC for help with the experiments.

This work was supported by National Institutes of Health grants HL076604 and DK077762, as well as Deutsche Forschungsgemeinschaft KFO 142 grants GE2063/1 (to H.G.) and GU769/1-3 and GU769/2-1 (to M.G.), and EU FP6 (NEST, Mamocell; to M.G.). H.G. is a New Investigator in Aging of the Ellison Medical Foundation.

Authorship

Contribution: A.K., M.-D.F., M.A.R., and D.D. performed most of the experiments; V.S. developed the algorithm to determine cell protrusion movement in vivo; and M.G. and H.G. performed experiments, planned and supervised all experiments, and wrote the manuscript.

Conflict-of-interest disclosure: The authors declare no competing financial interests.

Correspondence: Hartmut Geiger, Aging Research, KFO 142, Department of Dermatology and Allergic Diseases, University of Ulm, James Franck-Ring 11c, 89081 Ulm, Germany; e-mail: hartmut.geiger@uni-ulm.de; or Matthias Gunzer, Institute of Molecular and Clinical Immunology, Otto von Guericke University, Leipziger Str 44, 39120 Magdeburg, Germany; e-mail: matthias.gunzer@med.ovgu.de.

References

1. Korbling M, Estrov Z. Adult stem cells for tissue repair: a new therapeutic concept? *N Engl J Med.* 2003;349:570-582.
2. Morrison SJ, Uchida N, Weissman IL. The biology of hematopoietic stem cells. *Annu Rev Cell Dev Biol.* 1995;11:35-71.
3. Suda T, Arai F, Hirao A. Hematopoietic stem cells and their niche. *Trends Immunol.* 2005;26:426-433.
4. Yin T, Li L. The stem cell niches in bone. *J Clin Invest.* 2006;116:1195-1201.
5. Adams GB, Scadden DT. The hematopoietic stem cell in its place. *Nat Immunol.* 2006;7:333-337.
6. Lo Celso C, Fleming HE, Wu JW, et al. Live-animal tracking of individual haematopoietic stem/progenitor cells in their niche. *Nature.* 2009;457:92-96.
7. Xie Y, Yin T, Wiegraebe W, et al. Detection of functional haematopoietic stem cell niche using real-time imaging. *Nature.* 2009;457:97-101.
8. Li L, Neaves WB. Normal stem cells and cancer stem cells: the niche matters. *Cancer Res.* 2006;66:4553-4557.
9. Wilson A, Trumpp A. Bone-marrow haematopoietic-stem-cell niches. *Nat Rev Immunol.* 2006;6:93-106.
10. Geiger H, Van Zant G. The aging of lympho-hematopoietic stem cells. *Nat Immunol.* 2002;3:329-333.
11. Van Zant G, Liang Y. The role of stem cells in aging. *Exp Hematol.* 2003;31:659-672.
12. Rando TA. Stem cells, ageing and the quest for immortality. *Nature.* 2006;441:1080-1086.
13. Rossi DJ, Bryder D, Zahn JM, et al. Cell intrinsic alterations underlie hematopoietic stem cell aging. *Proc Natl Acad Sci U S A.* 2005;102:9194-9199.
14. Bell DR, Van Zant G. Stem cells, aging, and cancer: inevitabilities and outcomes. *Oncogene.* 2004;23:7290-7296.
15. Geiger H, Rennebeck G, Van Zant G. Regulation of hematopoietic stem cell aging in vivo by a distinct genetic element. *Proc Natl Acad Sci U S A.* 2005;102:5102-5107.
16. Chen J. Senescence and functional failure in hematopoietic stem cells. *Exp Hematol.* 2004;32:1025-1032.
17. Rossi DJ, Jamieson CH, Weissman IL. Stems cells and the pathways to aging and cancer. *Cell.* 2008;132:681-696.
18. Lansdorp PM. Telomeres, stem cells, and hematology. *Blood.* 2008;111:1759-1766.
19. Xing Z, Ryan MA, Daria D, et al. Increased hematopoietic stem cell mobilization in aged mice. *Blood.* 2006;108:2190-2197.
20. Geiger H, Koehler A, Gunzer M. Stem cells, aging, niche, adhesion and Cdc42: a model for changes in cell-cell interactions and hematopoietic stem cell aging. *Cell Cycle.* 2007;6:884-887.
21. Jung S, Aliberti J, Graemmel P, et al. Analysis of fractalkine receptor CX(3)CR1 function by targeted deletion and green fluorescent protein reporter gene insertion. *Mol Cell Biol.* 2000;20:4106-4114.
22. Geiger H, True JM, Grimes B, Carroll EJ, Fleischman RA, Van Zant G. Analysis of the hematopoietic potential of muscle-derived cells in mice. *Blood.* 2002;100:721-723.
23. Gunzer M, Weishaupt C, Hillmer A, et al. A spectrum of biophysical interaction modes between T cells and different antigen-presenting cells during priming in 3-D collagen and in vivo. *Blood.* 2004;104:2801-2809.
24. Niesner R, Andresen V, Neumann J, Spiecker H, Gunzer M. The power of single and multibeam two-photon microscopy for high-resolution and high-speed deep tissue and intravital imaging. *Biophys J.* 2007;93:2519-2529.
25. Niesner RA, Andresen V, Gunzer M. Intravital two-photon microscopy: focus on speed and time resolved imaging modalities. *Immunol Rev.* 2008;221:7-25.
26. Reichardt P, Gunzer F, Gunzer M. Analyzing the physicodynamics of immune cells in a three-dimensional collagen matrix. *Methods Mol Biol.* 2007;380:253-269.
27. Filippi MD, Harris CE, Meller J, Gu Y, Zheng Y, Williams DA. Localization of Rac2 via the C terminus and aspartic acid 150 specifies superoxide generation, actin polarity and chemotaxis in neutrophils. *Nat Immunol.* 2004;5:744-751.

28. Szczur K, Xu H, Atkinson S, Zheng Y, Filippi MD. Rho GTPase CDC42 regulates directionality and random movement via distinct MAPK pathways in neutrophils. *Blood.* 2006;108:4205-4213.
29. Chan CK, Chen CC, Luppen CA, et al. Endochondral ossification is required for haematopoietic stem-cell niche formation. *Nature.* 2009;457:490-494.
30. Sipkins DA, Wei X, Wu JW, et al. In vivo imaging of specialized bone marrow endothelial microdomains for tumor engraftment. *Nature.* 2005;435:969-973.
31. Colmone A, Amorim M, Pontier AL, Wang S, Jablonski E, Sipkins DA. Leukemic cells create bone marrow niches that disrupt the behavior of normal hematopoietic progenitor cells. *Science.* 2008;322:1861-1865.
32. Junt T, Schulze H, Chen Z, et al. Dynamic visualization of thrombopoiesis within bone marrow. *Science.* 2007;317:1767-1770.
33. Lindquist RL, Shakhar G, Dudziak D, et al. Visualizing dendritic cell networks in vivo. *Nat Immunol.* 2004;5:1243-1250.
34. Auffray C, Fogg D, Garfa M, et al. Monitoring of blood vessels and tissues by a population of monocytes with patrolling behavior. *Science.* 2007;317:666-670.
35. Suzuki N, Ohneda O, Minegishi N, et al. Combinatorial Gata2 and Sca1 expression defines hematopoietic stem cells in the bone marrow niche. *Proc Natl Acad Sci U S A.* 2006;103:2202-2207.
36. Sapoznikov A, Pewzner-Jung Y, Kalchenko V, Krauthgamer R, Shachar I, Jung S. Perivascular clusters of dendritic cells provide critical survival signals to B cells in bone marrow niches. *Nat Immunol.* 2008;9:388-395.
37. Huang D, Shi FD, Jung S, et al. The neuronal chemokine CX3CL1/fractalkine selectively recruits NK cells that modify experimental autoimmune encephalomyelitis within the central nervous system. *FASEB J.* 2006;20:896-905.
38. Niess JH, Brand S, Gu X, et al. CX3CR1-mediated dendritic cell access to the intestinal lumen and bacterial clearance. *Science.* 2005;307:254-258.
39. Gunzer M, Friedl P, Niggemann B, Brocker EB, Kampgen E, Zanker KS. Migration of dendritic cells within 3-D collagen lattices is dependent on tissue origin, state of maturation, and matrix structure and is maintained by proinflammatory cytokines. *J Leukocyte Biol.* 2000;67:622-629.
40. Adams GB, Chabner KT, Alley IR, et al. Stem cell engraftment at the endosteal niche is specified by the calcium-sensing receptor. *Nature.* 2006;439:599-603.
41. Nilsson SK, Johnston HM, Coverdale JA. Spatial localization of transplanted hemopoietic stem cells: inferences for the localization of stem cell niches. *Blood.* 2001;97:2293-2299.
42. Daria D, Filippi MD, Knudsen ES, et al. The retinoblastoma tumor suppressor is a critical intrinsic regulator for hematopoietic stem and progenitor cells under stress. *Blood.* 2008;111:1894-1902.
43. Tanentzapf G, Devenport D, Godt D, Brown NH. Integrin-dependent anchoring of a stem-cell niche. *Nat Cell Biol.* 2007;9:1413-1418.
44. Orschell-Traycoff CM, Hiatt K, Dagher RN, Rice S, Yoder MC, Srour EF. Homing and engraftment potential of Sca-1$^+$lin$^-$ cells fractionated on the basis of adhesion molecule expression and position in cell cycle. *Blood.* 2000;96:1380-1387.
45. Prosper F, Verfaillie CM. Regulation of hematopoiesis through adhesion receptors. *J Leukocyte Biol.* 2001;69:307-316.
46. Jung Y, Wang J, Havens A, Sun Y, Jin T, Taichman RS. Cell-to-cell contact is critical for the survival of hematopoietic progenitor cells on osteoblasts. *Cytokine.* 2005;32:155-162.
47. Rasin MR, Gazula VR, Breunig JJ, et al. Numb and Numbl are required for maintenance of cadherin-based adhesion and polarity of neural progenitors. *Nat Neurosci.* 2007;10:819-827.
48. Sakai T, Li S, Docheva D, et al. Integrin-linked kinase (ILK) is required for polarizing the epiblast, cell adhesion, and controlling actin accumulation. *Genes Dev.* 2003;17:926-940.
49. Gourlay CW, Ayscough KR. The actin cytoskeleton: a key regulator of apoptosis and ageing? *Nat Rev Mol Cell Biol.* 2005;6:583-589.
50. Friedl P, den Boer AT, Gunzer M. Tuning immune responses: diversity and adaptation of the immunological synapse. *Nat Rev Immunol.* 2005;5:532-545.
51. Gunzer M, Schafer A, Borgmann S, et al. Antigen presentation in extracellular matrix: interactions of T cells with dendritic cells are dynamic, short lived, and sequential. *Immunity.* 2000;13:323-332.
52. Henrickson SE, Mempel TR, Mazo IB, et al. T cell sensing of antigen dose governs interactive behavior with dendritic cells and sets a threshold for T cell activation. *Nat Immunol.* 2008;9:282-291.
53. Mempel TR, Henrickson SE, Von Andrian UH. T-cell priming by dendritic cells in lymph nodes occurs in three distinct phases. *Nature.* 2004;427:154-159.
54. Scadden DT. The stem-cell niche as an entity of action. *Nature.* 2006;441:1075-1079.
55. Cohen-Kaminsky S, Bousso P, Gunzer M. Imaging the immunological synapse. *Eur J Immunol.* 2007;37:299-300.
56. Reichardt P, Dornbach B, Gunzer M. The molecular makeup and function of regulatory and effector synapses. *Immunol Rev.* 2007;218:165-177.
57. Delon J, Stoll S, Germain RN. Imaging of T-cell interactions with antigen presenting cells in culture and in intact lymphoid tissue. *Immunol Rev.* 2002;189:51-63.
58. Dar A, Kollet O, Lapidot T. Mutual, reciprocal SDF-1/CXCR4 interactions between hematopoietic and bone marrow stromal cells regulate human stem cell migration and development in NOD/SCID chimeric mice. *Exp Hematol.* 2006;34:967-975.
59. Sugiyama T, Kohara H, Noda M, Nagasawa T. Maintenance of the hematopoietic stem cell pool by CXCL12-CXCR4 chemokine signaling in bone marrow stromal cell niches. *Immunity.* 2006;25:977-988.
60. Chambers SM, Shaw CA, Gatza C, Fisk CJ, Donehower LA, Goodell MA. Aging hematopoietic stem cells decline in function and exhibit epigenetic dysregulation. *PLoS Biol.* 2007;5:e201.
61. Kamminga LM, de Haan G. Cellular memory and hematopoietic stem cell aging. *Stem Cells.* 2006;24:1143-1149.
62. Kiel MJ, Yilmaz OH, Iwashita T, Terhorst C, Morrison SJ. SLAM family receptors distinguish hematopoietic stem and progenitor cells and reveal endothelial niches for stem cells. *Cell.* 2005;121:1109-1121.
63. Kiel MJ, Morrison SJ. Maintaining hematopoietic stem cells in the vascular niche. *Immunity.* 2006;25:862-864.
64. Wierenga PK, Weersing E, Dontje B, de Haan G, van Os R. Differential role for very late antigen-5 in mobilization and homing of hematopoietic stem cells. *Bone Marrow Transplant.* 2006;38:789-797.
65. Carstanjen D, Gross A, Kosova N, Fichtner I, Salama A. The $\alpha_4\beta_1$ and $\alpha_5\beta_1$ integrins mediate engraftment of granulocyte-colony-stimulating factor-mobilized human hematopoietic progenitor cells. *Transfusion.* 2005;45:1192-1200.
66. Wagers AJ, Allsopp RC, Weissman IL. Changes in integrin expression are associated with altered homing properties of Lin$^{-/lo}$Thy1.1^{lo}Sca-1$^+$c-*kit*$^+$ hematopoietic stem cells following mobilization by cyclophosphamide/granulocyte colony-stimulating factor. *Exp Hematol.* 2002;30:176-185.
67. Humphries JD, Byron A, Humphries MJ. Integrin ligands at a glance. *J Cell Sci.* 2006;119:3901-3903.
68. Stier S, Ko Y, Forkert R, et al. Osteopontin is a hematopoietic stem cell niche component that negatively regulates stem cell pool size. *J Exp Med.* 2005;201:1781-1791.
69. Nilsson SK, Johnston HM, Whitty GA, et al. Osteopontin, a key component of the hematopoietic stem cell niche and regulator of primitive hematopoietic progenitor cells. *Blood.* 2005;106:1232-1239.
70. Chiang EY, Hidalgo A, Chang J, Frenette PS. Imaging receptor microdomains on leukocyte subsets in live mice. *Nat Methods.* 2007;4:219-222.
71. Cheng J, Turkel N, Hemati N, Fuller MT, Hunt AJ, Yamashita YM. Centrosome misorientation reduces stem cell division during ageing. *Nature.* 2008;456:599-604.
72. Sakaue-Sawano A, Kurokawa H, Morimura T, et al. Visualizing spatiotemporal dynamics of multicellular cell-cycle progression. *Cell.* 2008;132:487-498.

2009 114: 290-298
doi:10.1182/blood-2008-12-195644 originally published online April 8, 2009

Altered cellular dynamics and endosteal location of aged early hematopoietic progenitor cells revealed by time-lapse intravital imaging in long bones

Anja Köhler, Vince Schmithorst, Marie-Dominique Filippi, Marnie A. Ryan, Deidre Daria, Matthias Gunzer and Hartmut Geiger

Blood (print ISSN 0006-4971, online ISSN 1528-0020), is published weekly by the American Society of Hematology, 2021 L St, NW, Suite 900, Washington DC 20036.